metals

MDPI

Article

Effect of Aqueous Media on the Recovery of Scandium by Selective Precipitation

Bengi Yagmurlu [1,2,*], Carsten Dittrich [1] and Bernd Friedrich [2]

[1] MEAB Chemie Technik GmbH, 52068 Aachen, Germany; carsten@meab-mx.com
[2] RWTH Aachen, IME Institute of Process Metallurgy and Metal Recycling, 52056 Aachen, Germany; BFriedrich@metallurgie.rwth-aachen.de
* Correspondence: bengi@meab-mx.com; Tel.: +49-1575-4954583

Received: 9 April 2018; Accepted: 1 May 2018; Published: 3 May 2018

Abstract: This research presents a novel precipitation method for scandium (Sc) concentrate refining from bauxite residue leachates and the effect of aqueous media on this triple-stage successive precipitation process. The precipitation pattern and the precipitation behavior of the constituent elements was investigated using different precipitation agents in three major mineral acid media, namely, H_2SO_4, HNO_3, and HCl in a comparative manner. Experimental investigations showed behavioral similarities between HNO_3 and HCl media, while H_2SO_4 media was different from them because of the nature of the formed complexes. NH_4OH was found to be the best precipitation agent in every leaching media to remove Fe(III) with low Sc co-precipitation. To limit Sc loss from the system, Fe(III) removal was divided into two steps, leading to more than 90% of Fe(III) removal at the end of the process. Phosphate concentrates were produced in the final step of the precipitation process with dibasic phosphates which have a strong affinity towards Sc. Concentrates containing more than 50% of $ScPO_4$ were produced in each case from the solutions after Fe(III) removal, as described. A flow diagram of the selective precipitation process is proposed for these three mineral acid media with their characteristic parameters.

Keywords: bauxite residue; red mud; hydrometallurgy; recovery; scandium; precipitation

1. Introduction

The recent agreements and climate accords in reducing carbon emission and specified deadlines for automotive industries have placed light metals and alloys under the spotlight [1]. One of the reasons is the direct relation between a vehicle weight and its energy consumption. Scandium (Sc) is used as a tuning metal especially for aluminum alloys, which makes it one of the promising candidates for light-weight alloys [2]. It is, however, an extremely expensive element for widespread application in industrial usage at the moment [3]. As aluminum alloys with improved strength, thermal resistance, and weldability can be achieved with minor additions of Sc, improved oxygen-ion conductivity can also be attained in solid oxide fuel cells [4–6]. Hence, this metal was classified recently as a critical metal for the future, leading to a steep increase in its demand despite its price [7].

Unfortunately, Sc is widely dispersed in nature and generally has to be extracted from secondary raw materials or as a by-product of uranium, nickel laterite, or titanium pigment processing. Bauxite residue (i.e., red mud) is the by-product obtained through the Bayer Process, yielding approximately four billion tons, with a previously reported annual production of 160 million tons [8,9]. This alkaline waste can be considered as a valuable resource because of its metal content (Fe, Al, Ti, Sc, Rare earth elements (REEs), etc.). Therefore, the complete or partial valorization of bauxite residues (BR) has lately been of great interest [10–13].

Previously, complete or partial recovery of Sc from bauxite residues was reported to be achieved mainly by solvent extraction, ion exchange, or the combination of these two techniques, as a result of its low concentration in the leachates [14–20]. Zhang et al. recovered 91% of Sc from bauxite residue leachates by inorganic metal(IV)–phosphate ion exchangers, although Fe(III) was found to be an interfering ion in this process [20]. In another study, a newly developed supported ionic liquid phase (SILP) achieved almost complete Sc extraction, while showing a decreased efficiency in the presence of Fe(III) [14]. In all of these hydrometallurgical operations, the co-extraction of Fe, Al, and Ti became a problem, and intensive purification was required to produce a high-quality product.

In our previous work, a three-staged precipitation process was designed using a sulfuric acid media based on a selective Fe removal step by NH_4OH, since Fe is the most problematic element during Sc processing [21,22]. This was successively followed by selective Sc phosphate precipitation by $(NH_4)_2HPO_4$. As a result of this precipitation route, a Sc phosphate concentrate containing 65% Sc was synthesized from impure synthetic bauxite residue leach solutions. Nevertheless, the processing route must be tailored in relation to the geological presence of the bauxite residue, depending on different minerology and association of the phases. Hence, different mineral acids other than H_2SO_4, such as HNO_3 and HCl, were also tried for leaching bauxite residues.

In order to cover a wider range of bauxite residues as well as other waste-generating processes, such as Ti-pigment and Ni laterite production, the design of selective Sc precipitation route for bauxite residues has to be adapted to different mineral acid media. Thus, this paper investigates the effect of different aqueous media on the recovery of Sc by a selective precipitation method.

2. Materials and Methods

A bauxite residue sample was obtained from Aluminium of Greece, subjected to lithium borate fusion, and analyzed using inductively coupled plasma mass spectrometry, ICP-MS/AAS, as shown in Table 1.

Table 1. Chemical composition of the bauxite residue (LOI: Loss of ignition).

Major Compounds	wt. %	Minor Compounds	ppm
Fe	29.6	La	110
Al	8.6	Ce	380
Ca	8.3	Sc	120
Si	3.3	Nd	100
Ti	2.6	Y	80
Na	2.8		
Others	32.1		
LOI	12.7		
LOI: Loss on ignition			

Synthetic leach solutions were prepared considering pre-treatments before performing the selective precipitation. The expected leachate is the pregnant leach solutions (PLS) after the major part of Fe, Al, and Ti are recovered from the solution by both pyrometallurgical and hydrometallurgical methods. Hence, the synthetic solution mentioned in this study is predictive of the formation of the real PLS. The Sc and REEs concentrations were arranged to be higher than in the real PLS to clearly observe the precipitation behaviors of these elements. Additionally, the selective precipitation process was also tested directly on the real solutions, obtaining similar results as those observed in this study [21,23].

In addition to the major impurities present in the bauxite residue (e.g., Fe and Al), Nd and Y are also considered representative elements of light and heavy REEs within the synthetic PLS, since they have similar chemical properties as same sub-groups of REEs.

Synthetic solutions in chloride media were prepared by adding the required amount of reagent-grade $FeCl_3 \cdot 6H_2O$, $AlCl_3$, $Sc_2(SO_4)_3 \cdot 5H_2O$, $NdCl_3 \cdot 6H_2O$, and $YCl_3 \cdot 6H_2O$. In a similar manner, reagent-grade $Fe(NO_3)_3 \cdot 9H_2O$, $Al_2(SO_4)_3 \cdot 18H_2O$, $Sc_2(SO_4)_3 \cdot 5H_2O$, $NdCl_3 \cdot 6H_2O$, and $YCl_3 \cdot 6H_2O$ were

used to synthesize the solution in nitrate media. Sulfate and chloride salts were first precipitated as hydroxides and washed before being converted into the necessary forms, to avoid unwanted sulfate or chloride ions which can affect the precipitation yields by promoting complex formations in the aqueous solution. All precipitation solutions were prepared from reagent-grade salts. The concentrations of the precipitation agents were 12.5 wt. % for $CaCO_3$ (limestone) slurry, 1 mol/L for NaOH, NH_4OH, and KOH, and 1 mol/L for K_2HPO_4, $(NH_4)_2HPO_4$, and Na_2HPO_4.

In order to have comparative precipitation results, a composition similar to the one used in the sulfate media was chosen. The pH of both systems was set between 1.2 and 1.4 with the addition of the necessary amounts of HCl or HNO_3. The composition of the synthetic solutions is presented in Table 2.

Table 2. Composition of the synthetic solutions in HNO_3 and HCl media.

	Composition in HNO_3 Media (mg/L)	Composition in HCl Media (mg/L)
Al	340	348
Fe(III)	312	290
Sc	86	78
Y	108	96
Nd	101	105

The precipitation agents mentioned were carefully added using a precision burette into 50 mL of the synthetic PLS while monitoring pH and temperature. All experiments presented in this study were done at room temperature. For hydroxide precipitation, the agents were added until the target pH was attained under mild agitation, to reach homogeneity in the solution and to prevent local pH differences.

Precipitation solutions containing dibasic phosphates were prepared as 1 mol/L and added into the leach solutions starting with a stoichiometric amount, considering only scandium precipitation. In each step, the amount added was doubled until reaching 20 times of the stoichiometric amount.

The resulted suspension for each case was then stabilized and homogenized at a given pH and temperature for 2 h and subsequently filtered through fine filter paper via suction filtration. The separated solid residue was washed with distilled water and dried at 110 °C for 24 h. Both filtered solutions and solid residues were assayed.

The concentrations of the constituent ions of iron (Fe), aluminum (Al), scandium (Sc), yttrium (Y), and neodymium (Nd) were determined by microwave plasma optical emission spectroscopy (Agilent MP-AES 4100, Mulgrave, VIC, Australia). Each sample was prepared by adding 100 µL of cesium ionization buffer and 500 µL of ultrapure concentrated HNO_3 to 10 mL of solution. Quantitative analyses were performed at 371.993 nm, 396.152 nm, 361.383 nm, 371.029 nm, and 430.358 nm, corresponding to the spectral emission lines for Fe, Al, Sc, Y, and Nd respectively.

The pH measurements were performed using a WTW ProfiLine pH 197 series pH-meter with a Sentix 81 precision electrode. The pH meter was calibrated with standard technical buffering solutions at pH 2.00, 4.01, and 7.00 to achieve maximum sensitivity in pH measurements.

3. Results

We previously reported that more than 90% of Fe can be removed with negligible amount of Sc loss from sulfuric acid-based solutions by simply adding NH_4OH in a dual-staged precipitation process [22]. Furthermore, with a successive precipitation route which combines both hydroxide precipitation and phosphate precipitation, a Sc phosphate concentrate, which is easier to process, can be synthesized from sulfate-based aqueous solutions. Since Sc-containing liquors can also exist in chloride or nitrate media, the effect of those aqueous media on precipitation should be investigated. By this way, the successive precipitation process can be adapted to other major mineral acid media.

3.1. Precipitation in HNO_3 Media

3.1.1. Fe Removal Step

In all recovery and purification operations regarding scandium, iron was reported to be one of the most problematic elements. Thus, to propose an easier route to process scandium, iron content should be minimized in the solution beforehand. We determined that the easiest route to this purpose was the hydroxide precipitation. Limestone slurry, sodium hydroxide, potassium hydroxide, and ammonium hydroxide were chosen as precipitation solutions, and a wide range of pH values was examined with the addition of these hydroxide donors.

The precipitation trends of the constituent elements as hydroxides are shown in Figure 1. The precipitation of Fe(III) with the addition of limestone slurry took place in the pH range between 2.0 and 3.5. As it can be seen from Figure 1a, when Fe(III) precipitation was triggered, the co-precipitation of the other components was around 25–30%. In the case of NaOH and KOH addition to the system (Figure 1b,c respectively), a more distinctive Fe(III) precipitation was observed. Yet, the co-precipitation levels were relatively high, between 10% and 20%, when more than 90% of Fe(III) was removed. The addition of NH_4OH produced similar results as those described in the sulfate system. A distinctive Fe(III) precipitation resulting in low co-precipitation levels of the other components was observed (Figure 1d). When more than 95% of Fe was removed from the solution, less than 5% of Sc and REEs precipitated. In all cases, the precipitation order was Fe(III) > Sc > Al > Y ≈ Nd.

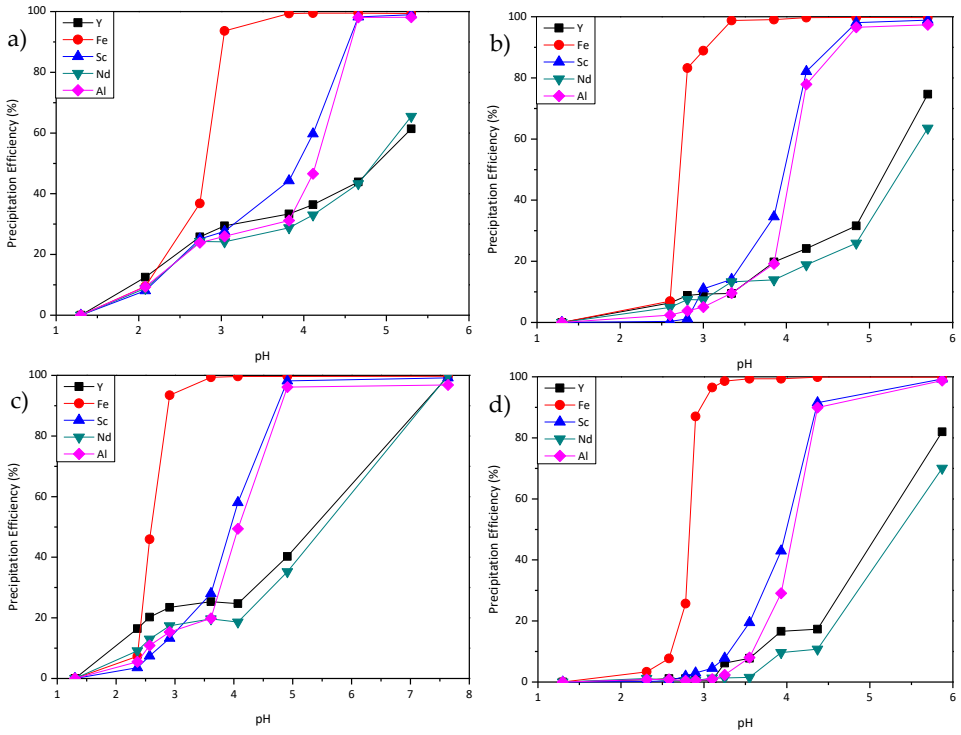

Figure 1. Precipitation behavior of Fe(III), Al, Sc, Nd, and Y in HNO_3 media at different pH values with the addition of (**a**) limestone; (**b**) NaOH; (**c**) KOH; (**d**) NH_4OH.

In this removal step, it is desirable to remove Fe from the system with minimum co-precipitation of the recoverable elements; therefore, selectivity was an essential parameter. The selectivity of the precipitation is calculated by Equation (1) given below:

$$D_{A,B} = \frac{C_{prec}}{C_{aq}} \text{ and } S_{A/B} = \frac{D_A}{D_B} \quad (1)$$

where D_A or D_B is the distribution coefficient of the mentioned element, C_{prec} is the concentration of the element in the precipitate, C_{aq} is the concentration of the element in the aqueous solution after precipitation, $S_{A/B}$ is the selectivity coefficient which indicates the selectivity of A over B.

The precipitation yields of the elements and the selectivity of Fe over Sc can be found in Table 3, when Fe precipitation reach 70% and 90%, respectively. Table 3a shows that the best candidates to remove Fe in HNO_3 media are NaOH and NH_4OH, since the corresponding $S_{Fe/Sc}$ values are far superior to those of the other hydroxide donors. Nevertheless, the co-precipitation levels of all elements abruptly increased in the case of NaOH upon further addition to remove 90% of Fe(III). Thus, NH_4OH showed an astonishing performance considering both the co-precipitation levels of the other elements and the $S_{Fe/Sc}$. Once that more than 95% of Fe present in the system was removed, around 4% of Sc and 1% of the other elements were precipitated with a remarkable $S_{Fe/Sc}$ of 585. The most logical explanation of this low co-precipitation levels is the occurrence of an hexamine scandium complex upon addition of NH_4OH [24,25]. Hence, Fe precipitation was triggered, whereas Sc remained in a complex form, which prevented the co-precipitation of Sc between these pH ranges.

The main difference of the nitrate-based aqueous solution compared to the sulfate-based one regards the pH ranges of the precipitation. Although it was found that the precipitation of Fe was triggered at pH values between 2.5 to 4.0 in sulfate media, a similar precipitation level was observed at a lower pH, between 2.0 to 3.0. It is known that sulfate ion form inner-sphere complexes, while nitrate complexes can be classified as forming outer-sphere complexes [26,27]. Consequently, more OH^- ions have to be released to disrupt inner-sphere complexes, since they have lower Gibbs Energy (ΔG) in that state.

Table 3. (a) Critical pH values for 70% Fe(III) removal from the system by hydroxide precipitation and precipitation % of the constituent ions with selectivity of Fe over Sc; (b) Critical pH values to obtain above 90% Fe(III) removal from the system by hydroxide precipitation and precipitation % of the constituent ions with selectivity of Fe over Sc.

(a)							
Precipitation Agent	**pH**	**Fe (%)**	**Sc (%)**	**Al (%)**	**Y (%)**	**Nd (%)**	**$S_{Fe/Sc}$**
Limestone	2.95	76.6	26.8	25.1	28.1	24.2	9
NaOH	2.78	72.3	1.1	3.3	8.1	6.8	235
KOH	2.74	69.7	10.4	13.1	21.9	15.2	20
NH_4OH (aq)	2.87	71.5	2.4	0.5	0.5	0.5	102
(b)							
Precipitation Agent	**pH**	**Fe (%)**	**Sc (%)**	**Al (%)**	**Y (%)**	**Nd (%)**	**$S_{Fe/Sc}$**
Limestone	3.05	93.6	27.6	25.9	29.4	24.2	38
NaOH	3.00	88.9	11.0	5.1	9.3	7.4	65
KOH	2.91	93.4	13.3	15.3	23.5	17.4	92
NH_4OH (aq)	3.10	96.5	4.5	0.9	0.6	1.3	585

3.1.2. Phosphate Precipitation

In previous studies, it was shown that there is a strong affinity of Sc and REEs for PO_4^{3-} ion [22,28,29]. In leach solutions with sulfate media, addition of dibasic phosphate resulted in a selective precipitation of both Fe(III) and Sc from the system. In light of this, dibasic phosphate solutions were tested with the intention of recovering Sc from the PLS. Addition of three different dibasic phosphate solutions and the resulting precipitation patterns of the constituent elements are shown in Figure 2. Precipitation solutions were added starting from the stoichiometric amount considering only Sc precipitation, and the amount introduced was increased in each step until reaching an amount 20 times greater than the stoichiometric value.

In all cases, similar precipitation trends were observed. Upon addition of the precipitant solution, immediate precipitation of Fe and Sc was initiated. More than 90% of Sc and Fe precipitation occurred at a pH value around 2.5. Since dibasic phosphates release OH^- into the system, an uncontrolled rise of pH would lead to the precipitation of the constituent elements as hydroxides, which will deteriorate the

selectivity towards Sc recovery. It is important to note that, while high levels of co-precipitation of the other elements were detected with Na_2HPO_4 addition, corresponding approximately to 40–50%, it was found that they were limited between 20% and 25% when K_2HPO_4 or $(NH_4)_2HPO_4$ were introduced into the solution as phosphate donors. In all cases, the additions yielded to the precipitation order Fe(III) = Sc > Al > Y = Nd. The precipitation efficiencies upon the addition of dibasic phosphate precipitation solutions can be found in Table 4.

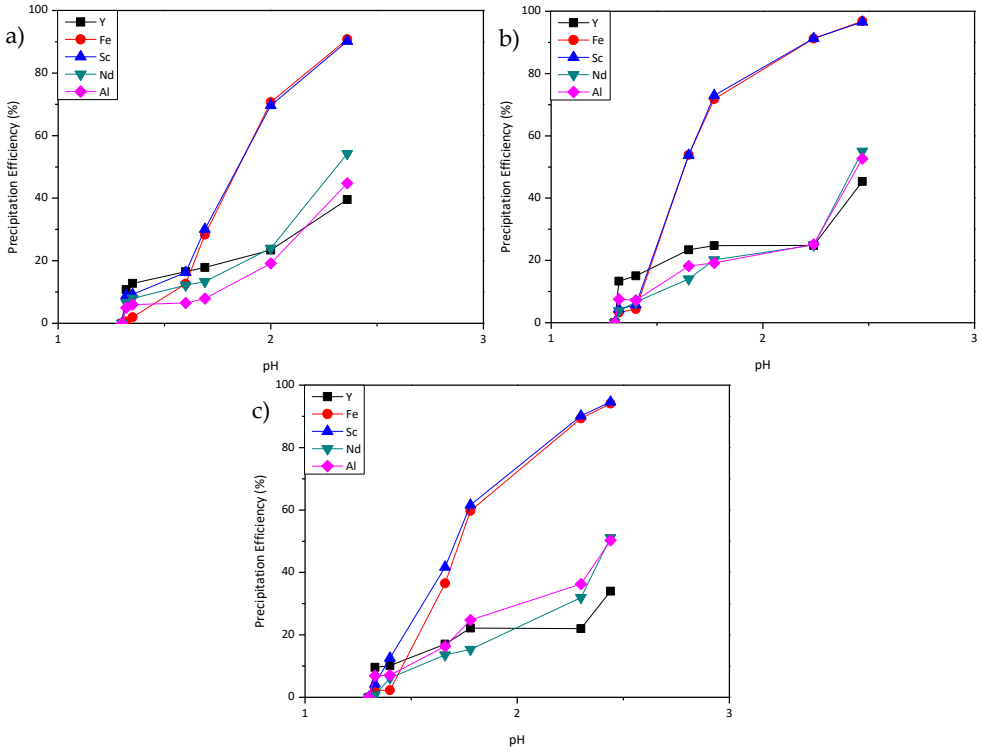

Figure 2. Precipitation of the elements in HNO_3 media with the addition of (**a**) Na_2HPO_4; (**b**) K_2HPO_4 and (**c**) $(NH_4)_2HPO_4$.

Table 4. Critical pH values for above 90% Sc recovery from the solution system by dibasic phosphate precipitation and precipitation efficiencies of the constituent ions.

Precipitation Agent	pH	Fe(III) (%)	Sc (%)	Al (%)	Y (%)	Nd (%)
Na_2HPO_4	2.36	90.8	90.2	44.8	39.6	54.3
K_2HPO_4	2.24	91.2	91.3	25.1	24.8	24.9
$(NH_4)_2HPO_4$	2.30	89.3	90.2	36.3	22.0	31.2

3.2. Precipitation in HCl Media

3.2.1. Fe Removal Step

The same precipitation solutions for hydroxide precipitation were further tested in HCl media, and the results are summarized in Figure 3. Similar precipitation routes and behaviors were observed as in the case of HNO_3 media. While the addition of limestone slurry resulted in the co-precipitation of all other elements with Fe(III), more distinctive cases were achieved when NaOH, KOH, and NH_4OH were used. As in the previous case, with the addition of NH_4OH, the lowest co-precipitation was achieved, yet Sc precipitation was observed to be the greatest among the other elements when the Fe content in the solution was minimized. In all cases, the precipitation order was Fe(III) > Sc > Al > Y = Nd.

The precipitation percentages of the elements in the solution can be found in Table 5, when Fe(III) was removed at 70% and 90%, respectively. The major difference in the precipitation behavior

between HNO_3 media and HCl media regarded the co-precipitation levels of Sc. It was previously discussed that both in nitrate and in sulfate media, Sc remained in the solution, while Fe(III) was almost completely taken out from the solution. With the addition of NH_4OH, 70% of Fe(III) as well as 9% of Sc were precipitated at pH values around 2.8, while Sc precipitation remained at 13% once 93% of Fe(III) was removed from the solution at a pH value around 3.0. The interaction between Fe^{3+} and Cl^- ions was the main reason why the precipitation level was limited, and the co-precipitation level of Sc increased when Fe started to precipitate. This interaction shifted the precipitation range of Fe(III) slightly, prompting Sc precipitation in the same range.

Still, the precipitation procedure to synthesize a scandium concentrate is applicable even in this case. Although the selectivity of Fe over Sc was found to be 24 when the precipitation of Fe reached 70%, as the precipitation progressed, a value of 100 was reached with the addition of NH_4OH.

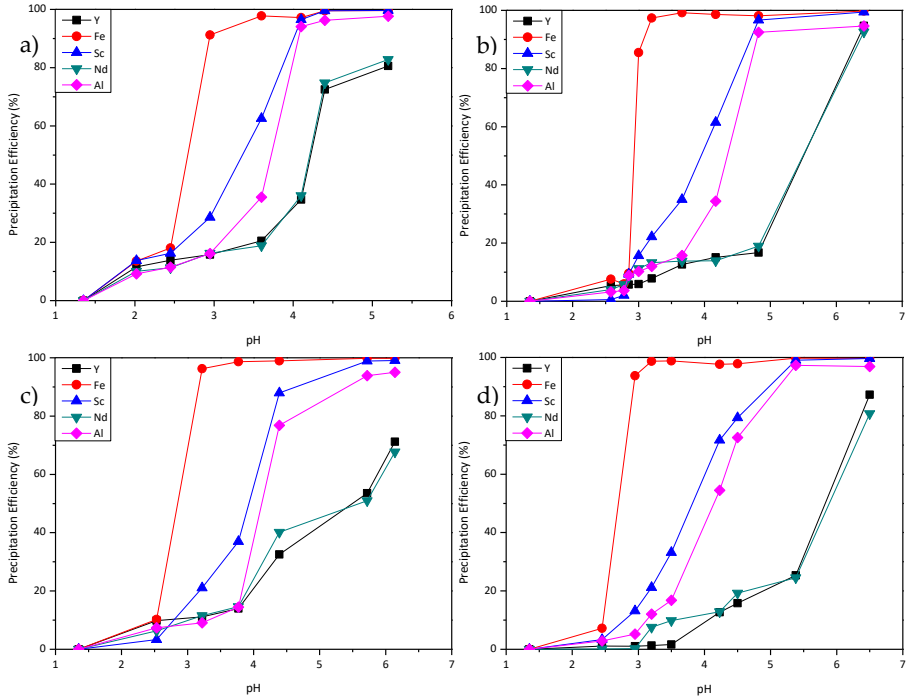

Figure 3. Precipitation behavior of Fe(III), Al, Sc, Nd, and Y in HCl media with the addition of (**a**) $CaCO_3$; (**b**) NaOH; (**c**) KOH; (**d**) NH_4OH.

Table 5. (a) Critical pH values for 70% Fe(III) removal from the system by hydroxide precipitation and precipitation % of the constituent ions with selectivity of Fe over Sc; (b) Critical pH values for above 90% Fe(III) removal from the system by hydroxide precipitation and precipitation % of the constituent ions with selectivity of Fe over Sc.

(a)							
Precipitation Agent	**pH**	**Fe (%)**	**Sc (%)**	**Al (%)**	**Y (%)**	**Nd (%)**	**$S_{Fe/Sc}$**
Limestone	2.81	70.7	25.2	15.3	15.1	15.6	7
NaOH	2.97	70.3	14.4	9.9	5.8	10.6	14
KOH	3.05	75.1	16.7	8.2	10.6	8.3	15
NH_4OH	2.82	71.3	9.6	4.4	1.0	0.2	24
(b)							
Precipitation Agent	**pH**	**Fe (%)**	**Sc (%)**	**Al (%)**	**Y (%)**	**Nd (%)**	**$S_{Fe/Sc}$**
Limestone	2.95	91.2	28.6	25.9	29.4	24.2	25
NaOH	3.10	91.4	18.9	11.1	6.9	12.3	46
KOH	3.22	96.3	21.0	9.1	11.1	11.5	98
NH_4OH	2.95	93.8	13.2	5.2	1.1	0.3	100

3.2.2. Phosphate Precipitation

Figure 4 shows the precipitation behavior with the addition of different phosphate donors into a synthetic solution with HCl media. The selective precipitations of scandium and iron were triggered immediately with the addition of a dibasic phosphate solution, and 60% precipitation efficiency was attained, with below 10% co-precipitation of other elements at pH values around 1.5 in all cases. After that point, further addition of phosphate ions resulted in the growth of both targeted and non-targeted elements. The best selectivity with 90% of Sc precipitation efficiency was reached at pH 2.2 with the addition of K_2HPO_4, with co-precipitation yields of 27%, 26%, and 43% for Al, Y, and Nd, respectively. $(NH_4)_2HPO_4$ showed a similar performance with slightly increased co-precipitation levels corresponding to 36% for Al, 23% for Y, and 42% for Nd when Sc precipitation hit 90%. Critical pH values for above 90% Sc recovery from the solution system by dibasic phosphate precipitation and the precipitation efficiencies of the constituent ions can be found in Table 6.

Since introducing new ions into the system is unwanted throughout the precipitation process, $(NH_4)_2HPO_4$ was selected as the best precipitation agent for selective precipitation of Sc from bauxite residue leachates.

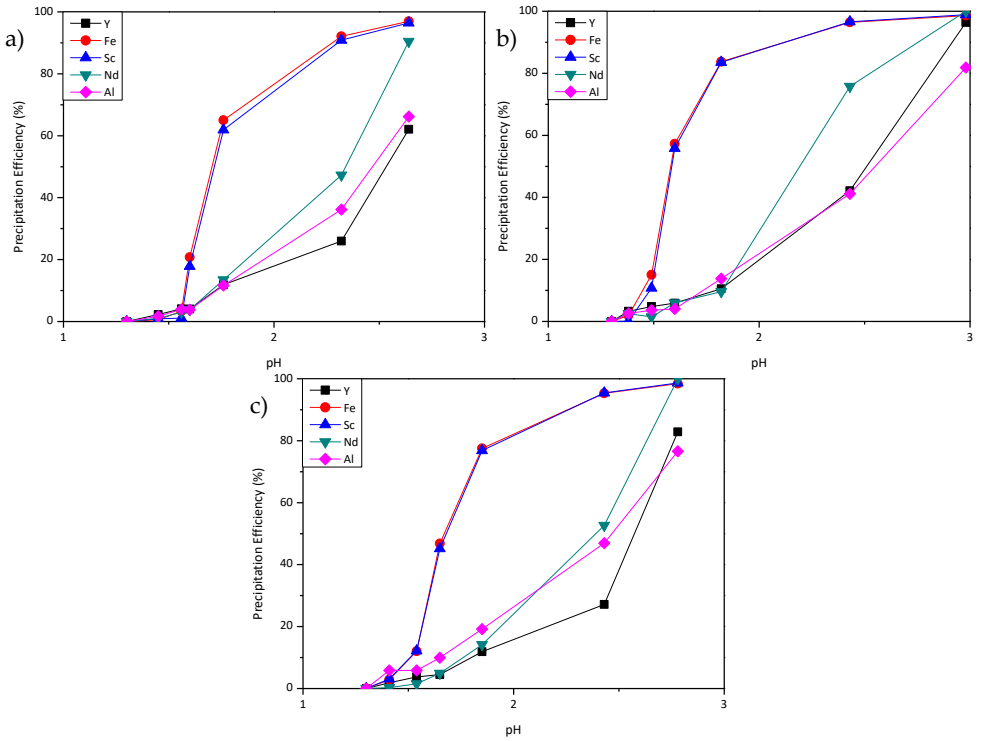

Figure 4. Precipitation of the elements in HCl media with the addition of (**a**) Na_2HPO_4; (**b**) K_2HPO_4 and (**c**) $(NH_4)_2HPO_4$.

Table 6. Critical pH values for above 90% Sc recovery from the solution system by dibasic phosphate precipitation and precipitation efficiencies of the constituent ions.

Precipitation Agent	pH	Fe(III) (%)	Sc (%)	Al (%)	Y (%)	Nd (%)
Na_2HPO_4	2.32	92.1	90.9	39.2	26.0	47.3
K_2HPO_4	2.19	90.1	90.2	27.5	26.3	42.7
$(NH_4)_2HPO_4$	2.27	90.4	90.3	36.3	22.9	42.1

3.3. Successive Precipitation in All Media

Taking all the findings into consideration, triple-staged precipitation processes for the synthesis of a scandium concentrate from bauxite residue solutions can be proposed using the described mineral

acid systems. The proposed precipitation processes are summarized in Figure 5, and the variation in concentration with the successive addition of the precipitation agents in H_2SO_4, HNO_3, and HCl media can be found in Figure 5a–c, respectively. Three precipitation regions labelled as regions 1, 2, and 3 are shown in all graphs. Region 1 is the removal of Fe from a solution with minimum Sc loss by the addition of NH_4OH until a specified pH is reached for each media. The residue obtained from this step, which was enriched in Fe, was filtered and removed from the solution. The critical pH ranges for the first Fe removal step were established as 3.3–3.4 for H_2SO_4 and 2.8–2.9 for HNO_3 and HCl. Region 2 denotes the second Fe removal step by further addition of NH_4OH that promotes higher Fe precipitation with a low amount of Sc co-precipitation. The precipitate was then filtered and could be recycled into the initial feed, which minimized Sc losses during the second Fe removal step and provided a seeding agent for better Fe separation. The pH ranges for this step were between 3.6–3.7 for H_2SO_4, 3.1–3.2 for HNO_3, and 3.0–3.1 for HCl media.

After removing more than 95% of Fe using NH_4OH with low Sc loss, a phosphate precipitation step was applied in the third part of this successive precipitation process. It was observed that the phosphate precipitation with dibasic phosphates showed similar performances regardless of the system. The pH of all systems was adjusted to 2.0 in advance, with the purpose to avoid unwanted hydroxide precipitation which can be triggered at pH levels above 3.0. Dibasic phosphate solutions were added into all systems until reaching a pH range between 2.5 and 2.6, where the best selectivity for Sc was reached. Since Fe was removed in previous steps, both the amount of precipitant solution and the co-precipitation levels of the constituent ions were decreased. For all media, more than 95% of Sc and Fe was recovered, while approximately 15% of Al and 10% of Y and Nd were co-precipitated during the process. The compositions of the resulted concentrate in the form of mixed phosphates can be found in Table 7.

Table 7. Compositions of each concentrate obtained after their successive selective precipitation as phosphates.

	H_2SO_4	**HNO_3**	**HCl**
$ScPO_4$ (%)	66	56	51
$FePO_4$ (%)	13	12	13
$AlPO_4$ (%)	19	23	26
YPO_4 (%)	1	3	5
$NdPO_4$ (%)	1	6	5

In all cases, Sc concentrates containing more than 50% $ScPO_4$ were synthesized. Since the precipitation patterns of the ions were more discrete in the sulfuric acid media, the best results were obtained in this media, with 66% $ScPO_4$. The major impurity element was found to be Al in the concentrate, which can be easily processed and removed with basic purification operations.

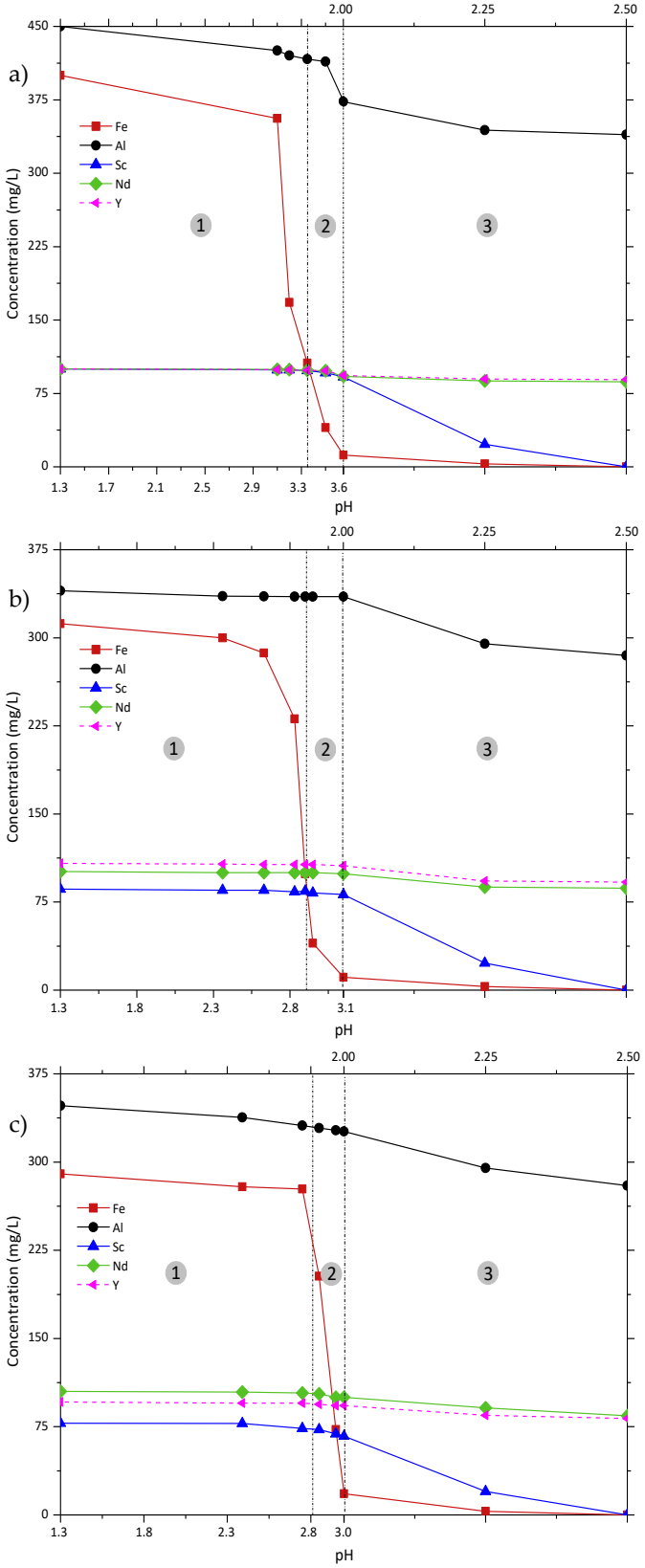

Figure 5. Triple-staged successive precipitation with NH_4OH and $(NH_4)_2HPO_4$ from (**a**) H_2SO_4; (**b**) HNO_3 and (**c**) HCl media.

4. Assessment and Conclusions

A triple-step precipitation route is proposed to refine a scandium concentrate from synthetic bauxite residue leachates, and the effect in aqueous media was investigated. In all media, NH_4OH showed better selectivity and performance than the other hydroxides, similar to the results obtained in H_2SO_4 media. While HNO_3 and HCl media showed quite similar patterns during precipitation, they differed with respect to the H_2SO_4 media, especially in the pH ranges of precipitation, because of the nature of the formed complexes. Although Sc loss during the Fe removal step in HCl media was observed to be relatively higher compared to the other cases as a result of the interaction between Fe^{3+} and Cl^- ions, still the concentrate contained more than 50% of Sc. The proposed selective precipitation route to produce $ScPO_4$ concentrate can be seen in Figure 6.

A scandium concentrate containing more than 50% of $ScPO_4$ was successfully obtained with this selective precipitation route from synthetic solutions. Depending on the impurity level, the aqueous media, and the initial composition of the feed solution, the amount of $ScPO_4$ in the synthesized concentrate could vary between 15% and 65%. Since the concentrate contained more scandium than the other elements, the processing and the purification of this concentrate will be much easier to perform. The removal of the most problematic element for scandium precipitation, which is iron, is the main obstacle for advanced processes to obtain a high-purity scandium product. Furthermore, the remaining solution after precipitation can be treated for further REEs recovery through other means.

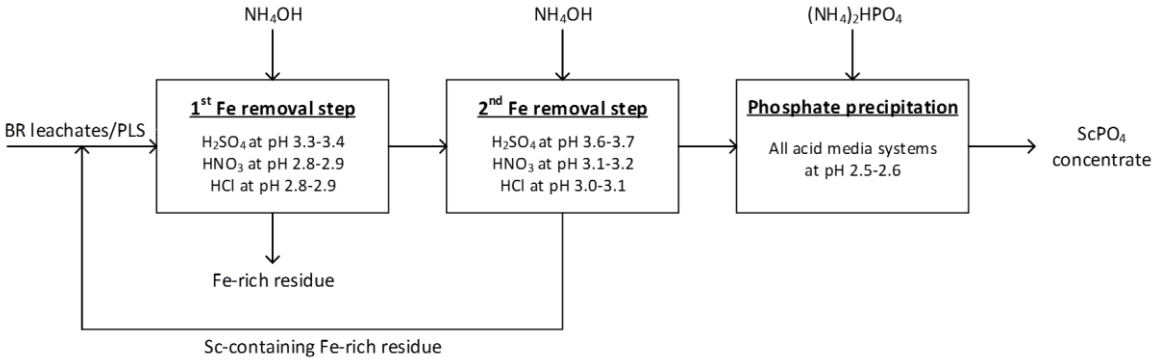

Figure 6. Proposed selective precipitation route to synthesize a $ScPO_4$ concentrate using three mineral acid media.

Author Contributions: B.Y., C.D., and B.F. conceived and designed the experiments; B.Y. performed the experiments; B.Y. analyzed the data; B.Y. wrote the paper; B.Y., C.D., and B.F. reviewed the paper.

Funding: This research was funded by European Community's Horizon 2020 Programme under grant agreement number 636876.

Acknowledgments: The research leading to these results has received funding from the European Community's Horizon 2020 Programme ([H2020/2014–2019]) under Grant Agreement no. 636876 (MSCA-ETN REDMUD). This publication reflects only the author's view, exempting the Community from any liability. Project website: http://www.etn.redmud.org. The authors thank Wenzhong Zhang and Dzenita Avdibegovic for their supports in ICP Measurements.

Conflicts of Interest: The authors declare no conflict of interest.

References

1. UNFCCC. Adoption of the Paris Agreement. Report No. FCCC/CP/2015/L.9/Rev.1. Available online: http://unfccc.int/resource/docs/2015/cop21/eng/l09r01.pdf (accessed on 15 January 2018).
2. Røyset, J.; Ryum, N. Scandium in aluminium alloys. *Int. Mater. Rev.* **2005**, *50*, 19–44. [CrossRef]
3. Gambogi, J. *USGS Minerals Information: Scandium*; U.S. Geological Survey: Reston, VA, USA; pp. 146–147.
4. Lathabai, S.; Lloyd, P. The effect of scandium on the microstructure, mechanical properties and weldability of a cast Al–Mg alloy. *Acta Mater.* **2002**, *50*, 4275–4292. [CrossRef]

5. Marquis, E.; Seidman, D. Nanoscale structural evolution of Al_3Sc precipitates in Al-Sc alloys. *Acta Mater.* **2001**, *49*, 1909–1919. [CrossRef]
6. Yamamoto, O. Solid oxide fuel cells: Fundamental aspects and prospects. *Electrochim. Acta* **2000**, *45*, 2423–2435. [CrossRef]
7. European Commission. *Study on the Review of the List of Critical Raw Materials: Executive Summary*; Directorate-General for Internal Market, Industry, Entrepreneurship and SMEs: Brussels, Belgium, 2017; pp. 1–93.
8. Power, G.; Gräfe, M.; Klauber, C. Bauxite residue issues: I. Current management, disposal and storage practices. *Hydrometallurgy* **2011**, *108*, 33–45. [CrossRef]
9. Evans, K. The history, challenges, and new developments in the management and use of bauxite residue. *J. Sustain. Metall.* **2016**, *2*, 316–331. [CrossRef]
10. Li, G.; Liu, M.; Rao, M.; Jiang, T.; Zhuang, J.; Zhang, Y. Stepwise extraction of valuable components from red mud based on reductive roasting with sodium salts. *J. Hazard. Mater.* **2014**, *280*, 774–780. [CrossRef] [PubMed]
11. Liu, Y.; Naidu, R. Hidden values in bauxite residue (red mud): Recovery of metals. *Waste Manag.* **2014**, *34*, 2662–2673. [CrossRef] [PubMed]
12. Paramguru, R.; Rath, P.; Misra, V. Trends in red mud utilization—A review. *Miner. Process. Extr. Metall. Rev.* **2004**, *26*, 1–29. [CrossRef]
13. Alkan, G.; Yagmurlu, B.; Cakmakoglu, S.; Hertel, T.; Kaya, Ş.; Gronen, L.; Stopic, S.; Friedrich, B. Novel approach for enhanced scandium and titanium leaching efficiency from bauxite residue with suppressed silica gel formation. *Sci. Rep.* **2018**, *8*, 5676. [CrossRef] [PubMed]
14. Avdibegović, D.; Regadío, M.; Binnemans, K. Recovery of scandium(III) from diluted aqueous solutions by a supported ionic liquid phase (silp). *RSC Adv.* **2017**, *7*, 49664–49674. [CrossRef]
15. Narayanan, R.P.; Kazantzis, N.K.; Emmert, M.H. Selective process steps for the recovery of scandium from jamaican bauxite residue (red mud). *ACS Sustain. Chem. Eng.* **2018**, *6*, 1478–1488. [CrossRef]
16. Ochsenkühn-Petropulu, M.; Lyberopulu, T.; Parissakis, G. Selective separation and determination of scandium from yttrium and lanthanides in red mud by a combined ion exchange/solvent extraction method. *Anal. Chim. Acta* **1995**, *315*, 231–237. [CrossRef]
17. Onghena, B.; Borra, C.R.; Van Gerven, T.; Binnemans, K. Recovery of scandium from sulfation-roasted leachates of bauxite residue by solvent extraction with the ionic liquid betainium bis (trifluoromethylsulfonyl) imide. *Sep. Purif. Technol.* **2017**, *176*, 208–219. [CrossRef]
18. Wang, W.; Cheng, C.Y. Separation and purification of scandium by solvent extraction and related technologies: A review. *J. Chem. Technol. Biotechnol.* **2011**, *86*, 1237–1246. [CrossRef]
19. Wang, W.; Pranolo, Y.; Cheng, C.Y. Recovery of scandium from synthetic red mud leach solutions by solvent extraction with D2HPA. *Sep. Purif. Technol.* **2013**, *108*, 96–102. [CrossRef]
20. Zhang, W.; Koivula, R.; Wiikinkoski, E.; Xu, J.; Hietala, S.; Lehto, J.; Harjula, R. Efficient and selective recovery of trace scandium by inorganic titanium phosphate ion-exchangers from leachates of waste bauxite residue. *ACS Sustain. Chem. Eng.* **2017**, *5*, 3103–3114. [CrossRef]
21. Yagmurlu, B.; Alkan, G.; Xakalashe, B.; Friedrich, B.; Stopic, S.; Dittrich, C. Combined saf smelting and hydrometallurgical treatment of bauxite residue for enhanced valuable metal recovery. In Proceedings of the 35th International Conference and Exhibition of ICSOBA, Hamburg, Germany, 2–5 October 2017.
22. Yagmurlu, B.; Dittrich, C.; Friedrich, B. Precipitation trends of scandium in synthetic red mud solutions with different precipitation agents. *J. Sustain. Metall.* **2017**, *3*, 90–98. [CrossRef]
23. Alkan, G.; Xakalashe, B.; Yagmurlu, B.; Kaussen, F.; Friedrich, B. Conditioning of red mud for subsequent titanium and scandium recovery–a conceptual design study. *World Metall. ERZMETALL* **2017**, *70*, 5–12.
24. Horovitz, C.T. *Scandium its Occurrence, Chemistry Physics, Metallurgy, Biology and Technology*; Elsevier: New York, NY, USA, 2012.
25. Vickery, R.C. *The Chemistry of Yttrium and Scandium*; Oxford: Oxford, UK, 1960; Volume 2.
26. Ahrland, S. How to distinguish between inner and outer sphere complexes in aqueous solution. Thermodynamic and other criteria. *Coord. Chem. Rev.* **1972**, *8*, 21–29. [CrossRef]
27. Spiro, T.G.; Revesz, A.; Lee, J. Volume changes in ion association reactions. Inner-and outer-sphere complexes. *J. Am. Chem. Soc.* **1968**, *90*, 4000–4006. [CrossRef]

28. Lucas, S.; Champion, E.; Bregiroux, D.; Bernache-Assollant, D.; Audubert, F. Rare earth phosphate powders $REPO_4 \cdot NH_2O$ (Re = La, Ce or Y)—Part i. Synthesis and characterization. *J. Solid State Chem.* **2004**, *177*, 1302–1311. [CrossRef]
29. Beltrami, D.; Deblonde, G.J.-P.; Bélair, S.; Weigel, V. Recovery of yttrium and lanthanides from sulfate solutions with high concentration of iron and low rare earth content. *Hydrometallurgy* **2015**, *157*, 356–362. [CrossRef]